Progress In Electromagnetics Research M, Vol. 84, 31–41, 2019

Optimum Design of Homopolar Radial Two-Degree-of-Freedom Hybrid Magnetic Bearing

Shengjing Yin*, Fengxiao Huang, Yukun Sun, Ye Yuan, Yonghong Huang, and Chi Chen

Abstract—Optimization design is a satisfactory way to improve the performance of magnetic bearing (MB). In this paper, a multi-objective genetic algorithm of particle swarm optimization (GAPSO) is proposed for homopolar permanent magnet biased magnetic bearings (HPRMBs). By assigning different inertia weights to each objective function, the multi-objective function is transformed into a new single objective function for optimization. In order to ensure the diversity of particles in the optimization process, genetic algorithm is used to cross-mutate them, which enhances the global search ability of particle swarm optimization. After optimization with GAPSO, the levitating force of the MB is increased by 22.3%, the volume decreased by 26.6%, and the loss reduced by 33.9%. The optimization results show that the multi-objective optimization based on GAPSO can effectively improve the performance of HPRMB.

1. INTRODUCTION

MB is a new type of support technology that uses non-contact magnetic force to stably suspend the rotor and has the advantages of no mechanical contact, no friction, no lubrication, long life, etc. [1–3]. It has been widely used in satellite attitude control, flywheel energy storage [4, 5], aerospace, high-speed high-precision machine tools, and vacuum ultra-clean [6].

MBs are generally divided into active magnetic bearings, passive magnetic bearings, and hybrid magnetic bearings [7, 8]. Hybrid magnetic bearing uses the bias magnetic flux generated by a permanent magnet to replace the bias magnetic flux generated by winding, which significantly reduces the loss of the MB [9–12]. HPRMB uses axial magnetization to generate bias flux, and permanent magnet generates the same polarity on a stator magnetic pole. This kind of MBs has smaller hysteresis loss on the rotor core, but the longer axial length limits the critical speed of a high-speed motor [13]. In order to improve the overall performance of MB, structural parameters should be optimized. The traditional optimization method mainly uses single-objective optimization by finite element software, in which calculation amount is large, and it is difficult to obtain an optimal solution for the mutual influence of objectives. In [14–17], MBs were optimized for single-objective optimization with volume, suspension force, and loss, respectively. Better results for single objective are obtained, but the other performance of the MB was degraded. Multi-objective evolutionary algorithm (MOEA) is used to optimize the axial hybrid magnetic bearing with biased permanent magnets in [18]. In [19], particle swarm optimization method was used to optimize radial magnetic bearings with volume and loss as optimization objectives, which obtained better optimization results. However, the above several optimization algorithms still use global optimization, which is easy to fall into local optimum in the optimization process, and the optimization efficiency is low. Therefore, it is necessary to find a fast convergence and global optimization algorithm for the design of MB. GAPSO is an optimization algorithm which combines

Received 17 June 2019, Accepted 1 August 2019, Scheduled 19 August 2019
* Corresponding author: Shengjing Yin (ysjlx0912@163.com).
The authors are with the School of Electrical and Information Engineering, Jiangsu University, Zhenjiang 212013, China.

genetic algorithm with particle swarm optimization. The algorithm has the advantages of strong global search ability, strong local search ability, fast convergence speed, and high running speed.

In this paper, GAPSO is used to optimize the structural parameters of HPRMB. Firstly, the mathematical model of bias magnetic circuit and control magnetic circuit is deduced by equivalent magnetic circuit method and verified by Ansys finite element method. Then, the suspension force, volume, and loss are selected as optimization objectives; the constraints and design variables are given; and the optimal structural parameters are obtained by GAPSO. Finally, the finite element is used to verify that the structure has good dynamic performance compared to the initial structure.

2. GENETIC PARTICLE SWARM OPTIMIZATION

The particle swarm optimization (PSO) algorithm is widely used to solve the problem of multi-objective optimization because of its advantages of easy implementation and fast optimization. PSO algorithm is proposed by Kennedy and Eberhart in 1995, an evolutionary algorithm based on swarm intelligence which originates from complex group behavior such as bird foraging [20, 21]. PSO first initializes a random particle swarm, and by calculating the fitness value of all particles, the individual optimal and global optimal values of the current particle are obtained. The updating of the position and velocity of the particles in flight is determined by both the individual and global optimum values, which leads to the continuous updating of individual optimum values and global optimum values of the particle swarm. The optimal solution of the asymptotic problem is approximated, and the optimal solution is finally obtained. The updating formulas of particle velocity and position are as follows:

$$v_{iD}^{k+1} = \omega v_{iD}^{k} + c_1 r_1 \left(p_{iD}^{k} - x_{iD}^{k}\right) + c_2 r_2 \left(p_{gD}^{k} - x_{gD}^{k}\right) \tag{1}$$

$$x_{iD}^{k+1} = x_{iD}^{k} + v_{iD}^{k+1} \tag{2}$$

where i is the particle number; k is the iteration number; c_1 and c_2 are learning factors; w is the inertia factor; p_i is the current individual optimal position; p_g is the current global optimal position; v_i is the current particle velocity.

However, the particle swarm is easy to fall into local optimum in the optimization process. In order to increase the diversity of the population and solve the local optimal problem of particle swarm, genetic algorithm is combined with particle swarm algorithm to generate GAPSO. This algorithm not only ensures powerful global search ability, but also integrates the position transfer idea of particle swarm. More efficiently, the obtained solution has higher precision and avoids the premature convergence of the particle swarm algorithm due to partial deadlock.

3. MODEL OF HPRMB

Figure 1 shows the structure of HPRMB. It can be seen from the figure that the magnetic circuit of HPRMB is composed of bias magnetic circuit and control magnetic circuit.

3.1. Suspension Calculation

The formula for calculating the suspension force of HPRMB is obtained from [22].

$$F_y = \frac{\phi^2}{\mu_0 S} = \frac{1}{\mu_0 S}\left[(\phi_{my-} + \phi_{cy-})^2 - (\phi_{my+} - \phi_{cy+})^2\right] \tag{3}$$

where F_y is the suspension force in Y direction, μ_0 the air permeability, S the magnetic pole area, ϕ_{my} the bias flux generated by the permanent magnet in Y directions, and ϕ_{cy} the control flux generated in Y directions.

Using the Taylor formula to linearize the above equation, the linearization equation for the rotor near the equilibrium position is

$$F(y, i_y) \cong \left.\frac{\partial F_y}{\partial y}\right|_{\substack{y=0 \\ i_y=0}} y + \left.\frac{\partial F_y}{\partial i}\right|_{\substack{y=0 \\ i_y=0}} i_y = k_y y + k_{iy} i_y \tag{4}$$

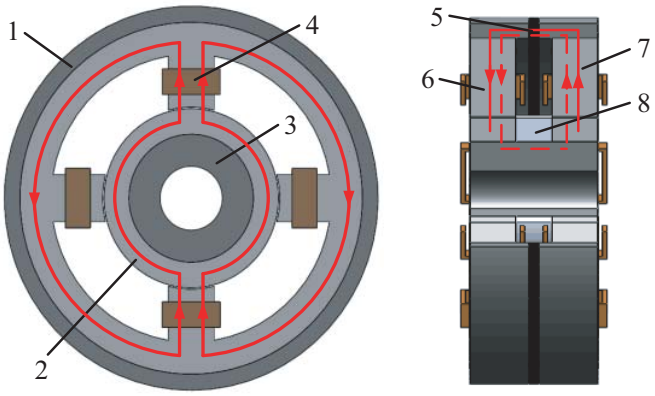

Figure 1. Structure of HPRMB. 1 — outer magnetic ring; 2 — rotor; 3 — inner magnetic conductor; 4 — control coil; 5 — permanent magnetic ring; 6 — left stator; 7 — right stator; 8 — magnetic isolation ring.

where k_i and k_y are the force-displacement stiffness and force-current stiffness near the equilibrium position in the Y direction, respectively. The two expressions are

$$k_y = \frac{F_m^2 \mu_0 S}{g_0 \left(2\mu_0 S R_{pm} + g_0\right)^2} \tag{5}$$

$$k_{iy} = \frac{2N_y F_m \mu_0 S}{g_0 \left(2R_{pm}\mu_0 S + g_0\right)} \tag{6}$$

Because of HPRMB with the same polarity, the formula of suspension force along the X axis can be obtained as follows

$$F_x \cong k_x x + k_{ix} i_x \tag{7}$$

where

$$k_x = \frac{F_m^2 \mu_0 S}{g_0 \left(2\mu_0 S R_{pm} + g_0\right)^2} \tag{8}$$

$$k_{ix} = \frac{2N_x F_m \mu_0 S}{g_0 \left(2R_{pm}\mu_0 S + g_0\right)} \tag{9}$$

3.2. Rationality Demonstration of Equivalent Magnetic Circuit

According to the design formula of magnetic bearing parameters in [19, 20] and the requirement of practical application, the initial model parameters of magnetic bearing designed in this paper are shown in Table 2.

The Ansys finite element method and analytical method are used to calculate the suspension force of the HPRMB with different rotor displacements and control currents. The correctness of the above mathematical model can be demonstrated by comparing the results. Figure 2 shows the suspension force curve obtained by the finite element method and the analytical method under different control currents. It can be seen from the figure that when the control current is $-4 \sim 4A$, the error of the results calculated by Ansys finite element method and analytical method is less than 5%, and the suspension force has a linear relationship with the control current. Figure 3 shows the relationship between the displacement and the suspension force obtained by the Ansys finite element method and analytical method under different rotor displacements. When the rotor is displaced, the error of suspension force calculated by finite element method and analytical method is between 0.2% and 5%.

The relative error rates above show good consistency of the curves obtained by the finite element method and analytical method. It can be observed from the curves that the suspension force is proportional to the control current and also proportional to the displacement of the rotor in the equilibrium position under the condition of unsaturated iron core.

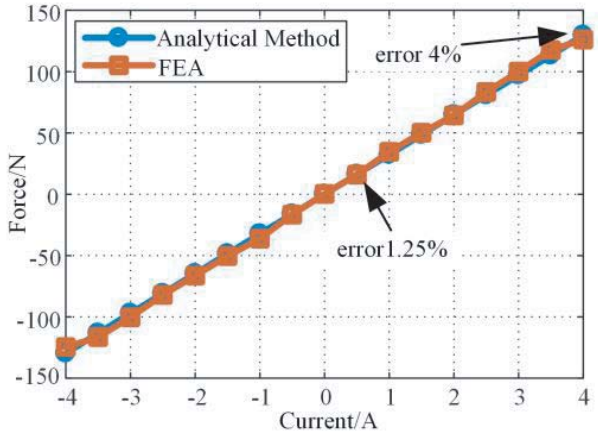

Figure 2. Current-force relationship.

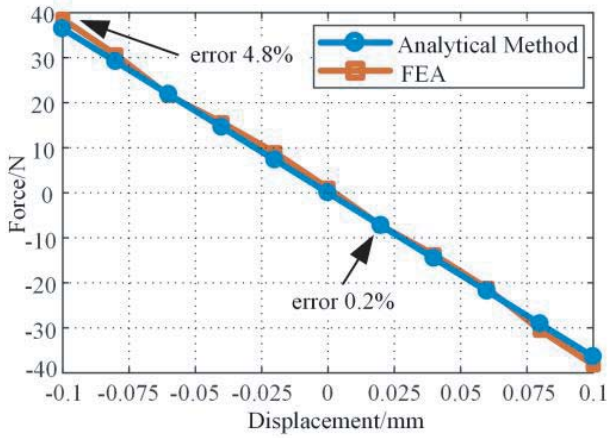

Figure 3. Displacement-force relationship.

4. OPTIMIZATION OF HPRMB

The main function of the magnetic suspension bearing is to provide enough suspension for the rotor. However, the increase of suspension force will inevitably lead to the increase of bearing volume and axial length. An increase in volume causes an increase in the loss of the bearing, and an increase in the axial length causes a decrease in the critical speed of the rotor. Therefore, it is necessary to multi-objectively optimize the HPRMB to have a small axial length, volume, and loss while ensuring sufficient levitation force.

4.1. Objective Function

The total volume expression of magnetic bearing is

$$\begin{aligned} V &= V_r + V_{ls} + V_{pm} + V_{rr} \\ &= \frac{\left(d_2^2 - d_1^2\right)}{4}\left(l_l + l_r + 2l_1 + l_{pm}\right)\pi + \frac{d_5^2 - d_4^2}{2} l_l \pi + 8(d_2 + g_0)\theta l \\ &\quad + \frac{\pi}{4}\left(d_6^2 - d_5^2\right) l_{pm} + \frac{\pi}{2}\left(d_6^2 - d_5^2\right)\left(l_1 + l_r\right) \end{aligned} \tag{10}$$

where V_r is the volume of the magnetic bearing rotor, V_{ls} the volume of the stator on the left side of the magnetic bearing, V_{pm} the volume of the permanent magnet, and V_{rs} the volume of the stator on the right side of the magnetic bearing.

The axial length of the magnetic bearing is expressed as

$$l = l_l + l_{pm} + 2l_1 + l_r \tag{11}$$

where l_r is the axial length of the right bearing, l_l the axial length of the left bearing, l_{pm} the axial length of the permanent magnet ring, and l_1 the axial length of the magnetic flux ring.

The expression of the eddy current loss of the magnetic bearing is

$$\begin{aligned} P_e &= \frac{1}{6\rho}\pi^2 e^2 f_r^2 B_m^2 V_{fe} \\ &= \frac{\pi^2 e^2 f_r^2 B_m^2}{6\rho} \times \left(\frac{d_5^2 - d_4^2}{2} l_l \pi + 8\theta l_r (d_2 + g_0) + \frac{(d_2^2 - d_1^2)}{4}(l_l + l_r + 2l_1 + l_{pm}) \right) \pi \end{aligned} \tag{12}$$

where ρ is the unit resistance of iron core, e the thickness of silicon steel sheet, f_r the re-magnetization frequency, B_m the maximum magnetic flux density, and V_{fe} the volume of iron core.

4.2. Selection of Optimization Variables

The design variables of magnetic bearing are shown in Figure 4 and Table 1, in which d_6, d_5, d_4, d_2, d_1, l_l, l_r, l_{pm}, l_1, θ, and g_0 are design variables. Because the rotor is rigid, the internal diameter of the rotor is calculated by modal method. d_3 can be expressed by rotor outer diameter d_2 and air gap g_0, so d_1 and d_3 are not considered as design variables. Considering the operating characteristics and manufacturing process of the magnetic bearing, the air gap length is 0.5 mm in this paper.

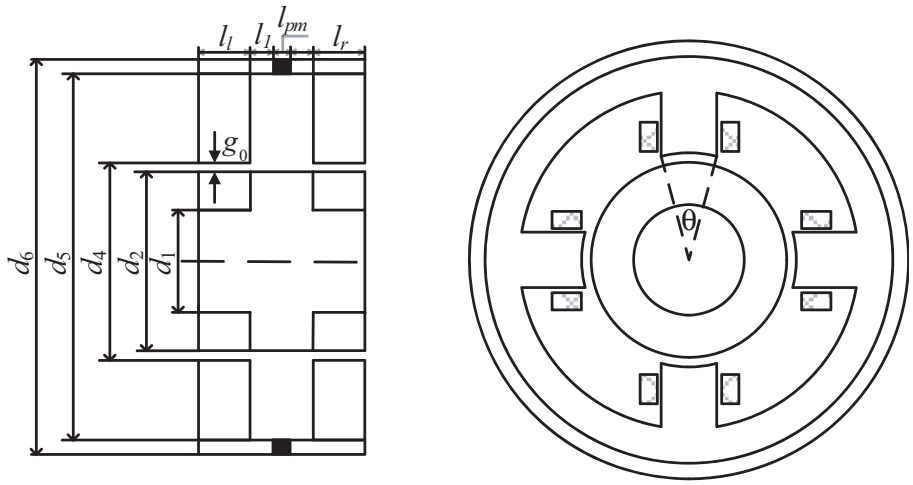

Figure 4. Design variables of HPRMB.

Table 1. Parameters and design variables.

Parameter	Design variable
outer diameter of stator	d_6
internal diameter of magnetic conduction ring	d_5
internal diameter of stator	d_4
outer diameter of rotor	d_2
internal diameter of rotor	d_1
axial length of left stator	l_l
axial length of right stator	l_r
thickness of permanent magnet	l_{pm}
pole arc of stator	θ

4.3. Constraints

According to the design experience, geometric rules and considering the actual application environment, the constraints of the magnetic suspension bearing design variables are as follows

$$\begin{cases} d_6 - d_5 > 0 & d_5 - d_4 > 0 & d_4 - d_3 > 0 \\ d_3 - d_2 > 0 & d_2 - d_1 > 0 & l_m - l_r < 0 \end{cases} \tag{13}$$

The saturated flux density of soft magnetic materials is 1.6 T. In order to avoid the saturation of soft magnetic materials, the maximum air gap flux density of magnetic bearings is set to 1.2 T. The air gap flux of magnetic bearings includes control flux and bias flux. When the suspension force of magnetic bearings reaches the maximum, the density of control flux and bias flux does not exceed 0.6 T.

Therefore, the constraints of flux density are

$$\begin{cases} B_c = \dfrac{Ni_{\max}\mu_0}{g_0} \leq 0.6 \\ B_m = \dfrac{6F_m\mu_0}{4\left(2\mu_0 SR_m + g_0\right)} \leq 0.6 \end{cases} \tag{14}$$

where B_c is the controlled flux density in X or Y direction, and B_m is the bias flux density generated by permanent magnets.

In order to ensure that the rotor can be stably suspended in the equilibrium position, the suspension force constraint is

$$F_y \geq 130 \tag{15}$$

Generally, there are weighted methods, goal programming methods, and Pareto optimal solution methods for multi-objective processing [21]. In this paper, the linear weighting method is used to assign the corresponding weights to each objective function, and the multi-objective function is transformed into a single objective to solve the problem. Multi-target conversion to a single objective function can be expressed as

$$F = \sum_{i=1}^{4} \omega_i f_i = \omega_1 V + \omega_2 l + \omega_3 P_e + \omega_4 F_y \tag{16}$$

The formula for calculating the ω_i of each objective function is as follows

$$\Delta_i = \frac{f_{i\max} - f_{i\min}}{2} \tag{17}$$

$$\omega_i = \frac{1}{\Delta_i^2} \tag{18}$$

where $f_{i\min}$ and $f_{i\max}$ are the minimum and maximum values of the objective function.

5. ANALYSIS OF OPTIMIZATION RESULTS

After determining the optimization objective function, design variables and constraints, main parameters of the GAPSO are set: the population size is 1000; the number of iterations of the particles is 10; the acceleration coefficients c_1 and c_2 are both 1.45. After 10 iterations, the Pareto optimal solution set is shown in Table 2.

Table 2. Design parameters of HPRMB.

Parameter	initial value1	initial value2	Optimization value
d_6/mm	120	120	112
d_5/mm	110	110	100
d_2/mm	28	28	26.7
g_0/mm	0.5	0.5	0.5
l_{pm}/mm	2	2.2	2.2
l_r/mm	12	12	10
θ	30	30	34.5
F/N	131	148.3	159
V/m^3	1.80E-4	1.80E-4	1.35E-4
P/W	13.72	14.1	9.07

As can be seen from the table, the initial design2 has an increased thickness of the permanent magnet compared to the initial design1, and the suspension force increases, but the loss of the MB also increases. Therefore, increasing the suspension force by merely increasing the thickness of the permanent

magnet does not optimize the performance of the bearing. It can be seen from the table that the comprehensive performance of HPRMB has been greatly improved after multi-objective optimization using GAPSO. The volume decreases from 1.80E-4m^3 to 1.35E-4m^3 with the rate 26.6% and axial length

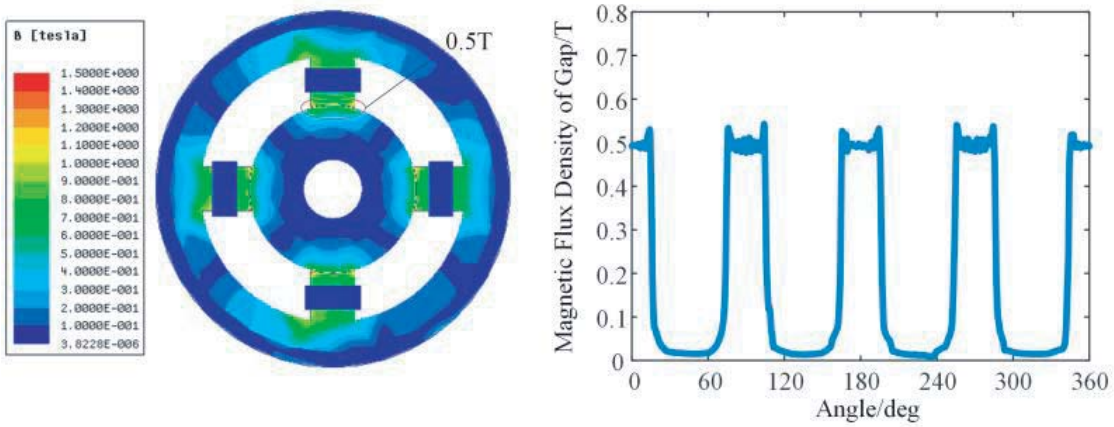

(a)

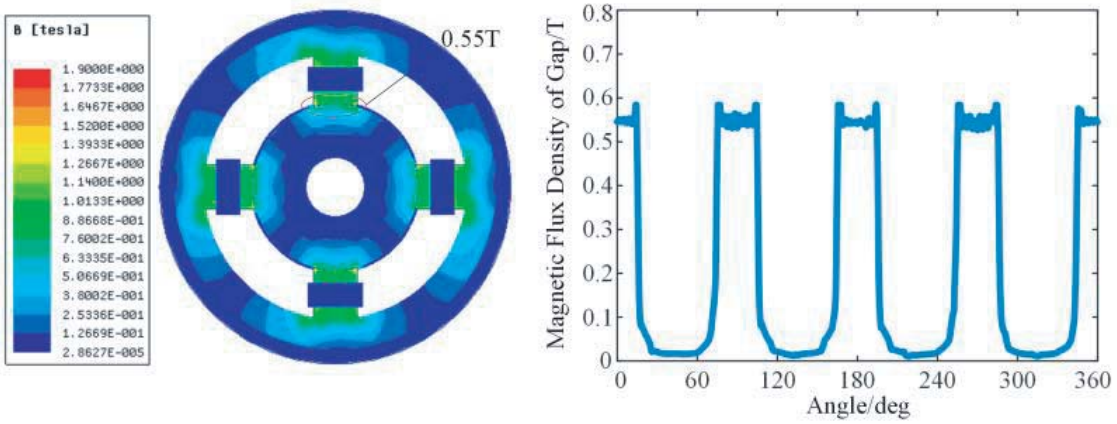

(b)

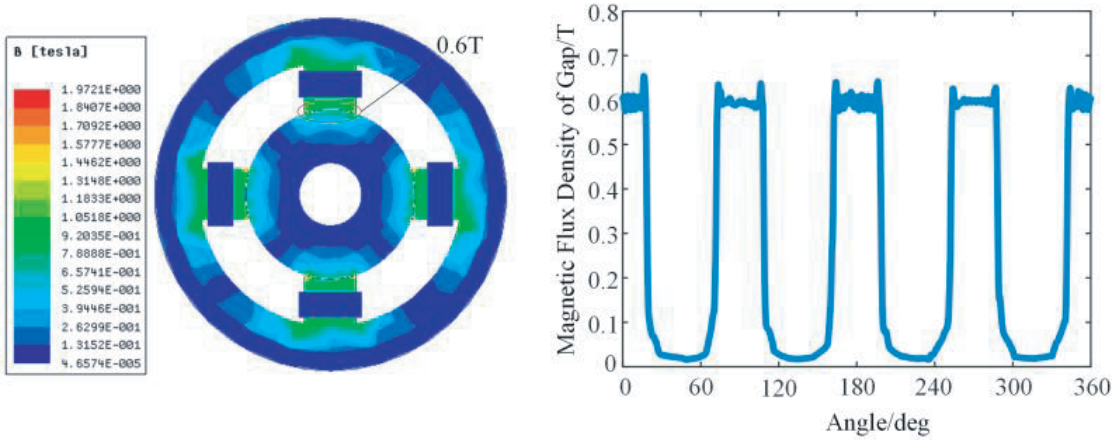

(c)

Figure 5. Distribution of bias magnetic flux density. (a) Initial design1. (b) Initial design2. (c) GAPSO design.

decreased from 29 mm to 25 mm. Compared with the initial design1, the suspension force is increased by 21.3% compared with the initial design2 by 7.2%, and the optimized magnetic bearing loss is reduced by 33.9% compared with the initial design1, which is lower than the initial design2 55.5%.

In order to verify the correctness and effectiveness of GAPSO, the distribution of magnetic flux density of HPRMB is calculated by Ansys finite element method. Figure 5 shows the magnetic density

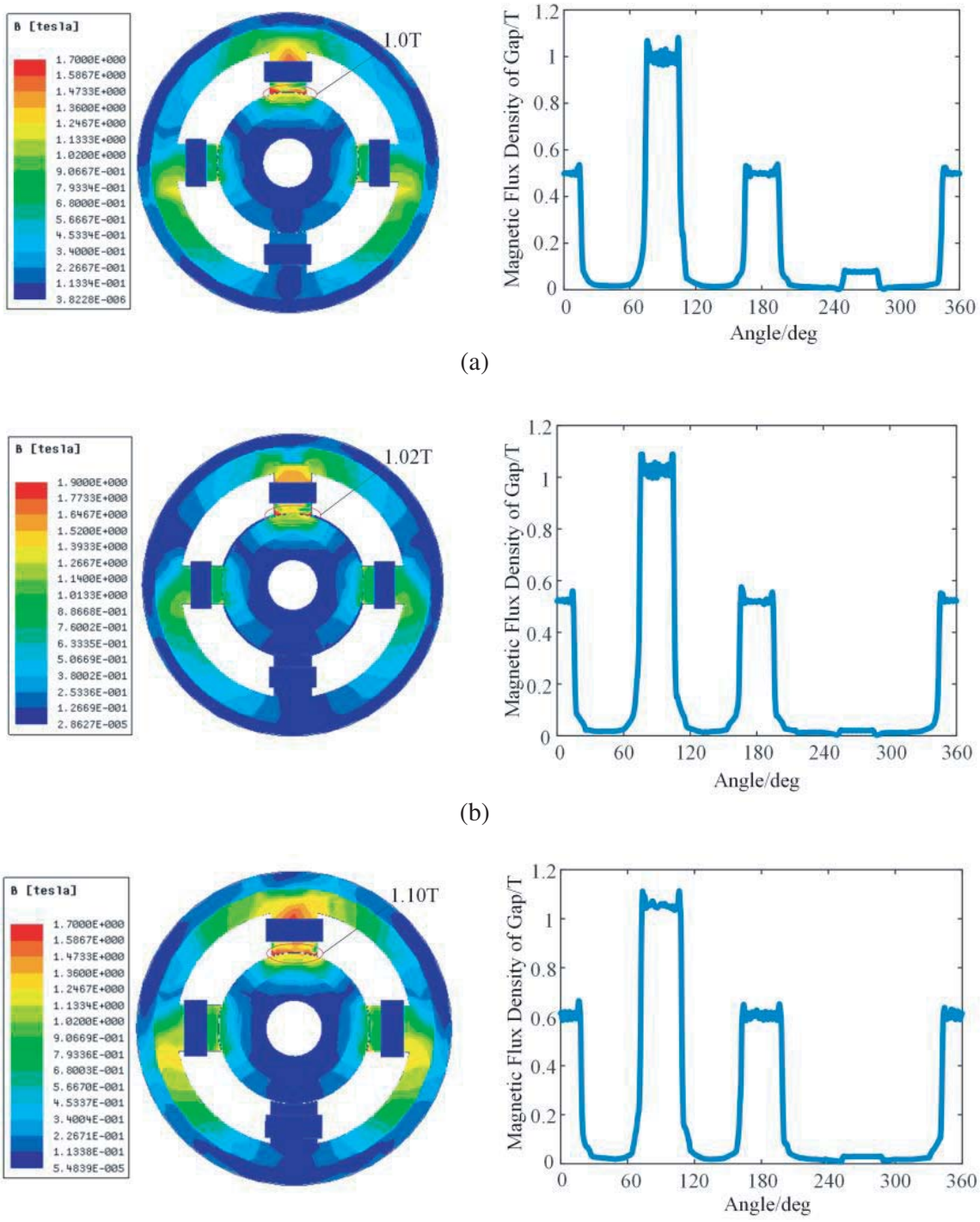

Figure 6. Distribution of magnetic flux density with maximum control current. (a) Initial design1. (b) Initial design1. (c) GAPSO design.

map of the bias magnetic flux before and after optimization. It can be seen from Figure 5 that the bias magnetic flux density of the initial design1 is about 0.5 T, the bias magnetic flux density of the initial design2 about 0.55 T, and the optimized bias magnetic flux density about 0.6 T.

The distribution of magnetic flux density of HPRMB of initial design and the GAPSO design with maximum control current are shown in Figure 6. It can be seen from Figure 6 that the synthetic magnetic flux density in the initial design1 air gap is about 1.0 T, the synthetic magnetic flux density in the initial design2 about 1.02 T, and the synthetic magnetic flux density in the optimized air gap about 1.10 T, which is less than the saturated flux density of soft-magnetic material 1.6 T.

Figure 7 shows the comparison of the variation of the suspension force with rotor displacement and control current before and after optimization. It can be seen from the figure that the suspension force is proportional to the displacement of the rotor and control current. After optimization, the current stiffness of the magnetic suspension bearing increases, and the displacement stiffness decreases. When the rotor of the bearing experiences the same displacement, the smaller displacement stiffness makes the required suspension force as the rotor returns to the equilibrium position. When the bearing is subjected to the same interference, the current stiffness is greater as the rotor returns to the equilibrium position. The smaller the current is, the smaller the loss is produced by the bearing. Therefore, the optimized magnetic suspension bearing has better dynamic performance than before optimization.

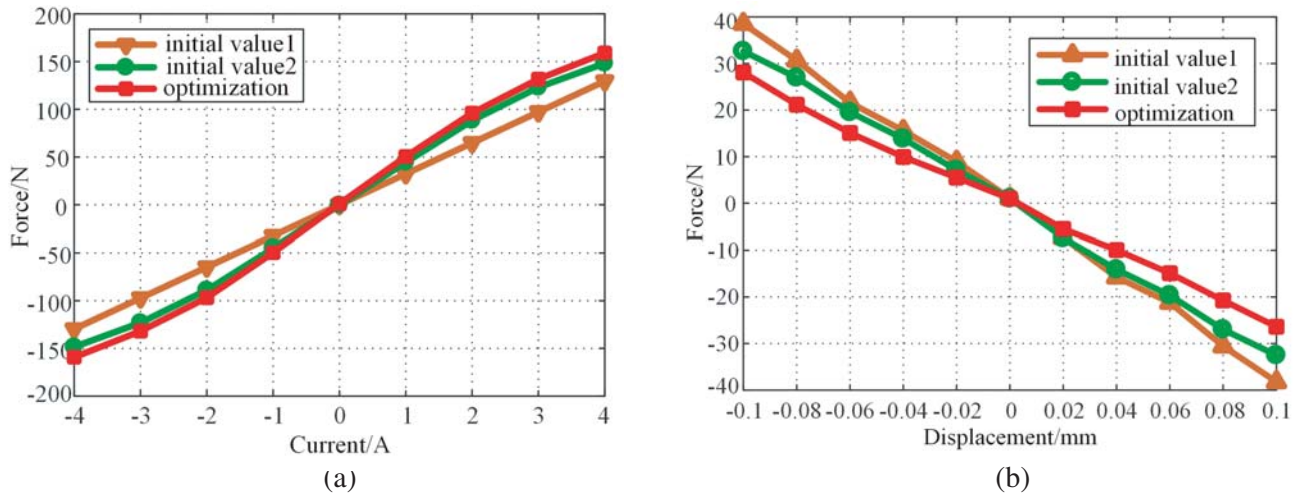

Figure 7. Current/displacement-force of initial design and GAPSO design. (a) Current-force relationship. (b) Displacement-force relationship.

6. CONCLUSION

In this paper, design and parameter optimization of the HPRMB is studied. The mathematical model of HPRMB is established by using equivalent magnetic circuit method, and its rationality is verified by Ansys finite element method. Then multi-objective optimization design of suspension force volume and loss is carried out by GAPSO. The optimization results show that the suspension force of the HPRMB is improved by 22.3%, the volume reduced by 26.6%, and the loss reduced by 33.9%. The performance of the HPRMB is greatly improved compared with the initial design. Compared with the Ansys finite element method, the GAPSO used in this paper has higher optimization efficiency, which has certain theoretical significance and practical engineering value.

ACKNOWLEDGMENT

This work was sponsored by the National Natural Science Foundation of China (51707082, 51877101) Natural Science Foundation of Jiangsu Province (BK20170546) and Priority Academic Program Development of Jiangsu Higher Education Institutions.

REFERENCES

1. Huang, Z., J. Fang, X. Liu, et al., "Loss calculation and thermal analysis of rotors supported by active magnetic bearings for high-speed permanent-magnet electrical machines," *IEEE Transactions on Industrial Electronics*, Vol. 63, No. 4, 2027–2035, 2016.
2. Zad, H. S., T. I. Khan, and I. Lazoglu, "Design and adaptive sliding mode control of hybrid magnetic bearings," *IEEE Transactions on Industrial Electronics*, Vol. 65, No. 3, 2537–2547, 2018.
3. Yuan, Y., Y. Sun, W. Zhang, et al., "Magnetic force numerical analysis of auxiliary bearings in optimized flywheel storage system," *Electric Machines and Control*, Vol. 20, No. 7, 95–101, 2016.
4. Han, B., S. Zheng, X. Wang, et al., "Integral design and analysis of passive magnetic bearing and active radial magnetic bearing for agile satellite application," *IEEE Transactions on Magnetics*, Vol. 48, No. 6, 1959–1966, 2012.
5. Nguyen, T. D. and G. Foo, "Sensorless control of a dual-airgap axial flux permanent magnet machine for flywheel energy storage system," *IET Electric Power Applications*, Vol. 7, No. 2, 140–149, 2013.
6. Han, B., S. Zheng, Y. Le, et al., "Modeling and analysis of coupling performance between passive magnetic bearing and hybrid magnetic radial bearing for magnetically suspended flywheel," *IEEE Transactions on Magnetics*, Vol. 49, No. 10, 5356–5370, 2013.
7. Zong, M., X. K. Wang, and Y. Cao, "Permanent magnet biased bearing of suspension system," *Advanced Materials Research*, Vols. 383–390, 5529–5535, 2011.
8. Han, B., S. Zheng, and H. Li, "Design and analysis of a two-axis-magnetic bearing with permanent magnet bias for magnetically suspended reaction wheel," *International Conference on Seventh International Conference on Intelligent System & Knowledge Engineering*, 2014.
9. Zhilichev, Y., "Analysis of a magnetic bearing pair with a permanent magnet excitation," *IEEE Transactions on Magnetics*, Vol. 36, No. 5, 3690–3692, 2000.
10. Mitterhofer, H., W. Gruber, and W. Amrhein, "On the high speed capacity of bearingless drives," *IEEE Transactions on Industrial Electronics*, Vol. 61, No. 6, 3119–3126, 2014.
11. Betschon, F., *Design Principles of Integrated Magnetic Bearings*, Swiss Federal Inst. Technol., Zurich, Switzerland, 2000.
12. Li, Z., H. Zhu, and X. Z, "Research on control system model of single degree of freedom hybrid magnetic bearing," *Journal of Nanjing University of Aeronautics & Astronautics*, Vol. 6, 685–690, 1998.
13. Wu, L., D. Wang, Z. Su, et al., "Analytical model of radial permanent magnet biased magnetic bearing with assist poles," *IEEE Transactions on Applied Superconductivity*, Vol. 26, No. 7, 1–5, 2016.
14. Moser, R., J. Sandtner, and H. Bleuler, "Optimization of repulsive passive magnetic bearings," *IEEE Transactions on Magnetics*, Vol. 42, No. 8, 2038–2042, 2006.
15. Zeisberger, M., T. Habisreuther, D. Litzkendorf, O. Surzhenko, R. Muller, and W. Gawalek, "Optimization of levitation forces in superconducting magnetic bearings," *IEEE Trans. Appl. Supercond.*, Vol. 11, No. 1, 1741–1744, Mar. 2001.
16. Sahinkaya, M. N. and A. E. Hartavi, "Variable bias current in magnetic bearings for energy optimization," *IEEE Transactions on Magnetics*, Vol. 43, No. 3, 1052–1060, Mar. 2007.
17. Shelke, S. and R. V. Chalam, "Optimum energy loss in electromagnetic bearing," *Proc. 3rd Int. Conf. Electron. Comput. Technol. (ICECT)*, 374–379, Kanyakumari, Tamil Nadu, Apr. 8–10, 2011.
18. Rao, J. S. and R. Tiwari, "Optimum design and analysis of axial hybrid magnetic bearings using multi-objective genetic algorithms," *International Journal for Computational Methods in Engineering Science & Mechanics*, 2012.
19. Liu, X. and B. Han, "The multiobjective optimal design of a two-degree-of-freedom hybrid magnetic bearing," *IEEE Transactions on Magnetics*, Vol. 50, No. 9, 1–14, 2014.
20. Han, B., Q. Xu, and Q. Yuan, "Multiobjective optimization of a combined radial-axial magnetic bearing for magnetically suspended compressor," *IEEE Transactions on Industrial Electronics*,

Vol. 63, No. 4, 2284–2293, 2016.

21. Kennedy, J. and R. Eberhaa, "Particle swarm optimization," *IEEE Int. Confon. Neural Networks*, 1942—1948, IEEE, Perth, USA, 1995.
22. Pichot, M. A., J. P. Kajs, B. R. Murphy, et al., "Active magnetic bearings for energy storage systems for combat vehicles," *IEEE Transactions on Magnetics*, Vol. 37, No. 1, 318–323, 2001.